



Queensland University of Technology
Brisbane Australia

This is the author's version of a work that was submitted/accepted for publication in the following source:

Frost, Ray L. & Xi, Yunfei (2012) A vibrational spectroscopic study of planchéite $\text{Cu}_8\text{Si}_8\text{O}_{22}(\text{OH})_4 \cdot \text{H}_2\text{O}$. *Spectrochimica Acta Part A : Molecular and Biomolecular Spectroscopy*, 91(June), pp. 314-318.

This file was downloaded from: <http://eprints.qut.edu.au/48988/>

© Copyright 2012 Elsevier

This is the author's version of a work that was accepted for publication in *Spectrochimica Acta Part A : Molecular and Biomolecular Spectroscopy*. Changes resulting from the publishing process, such as peer review, editing, corrections, structural formatting, and other quality control mechanisms may not be reflected in this document. Changes may have been made to this work since it was submitted for publication. A definitive version was subsequently published in *Spectrochimica Acta Part A : Molecular and Biomolecular Spectroscopy*, [VOL 91, ISSUE June, (2012)] DOI: 10.1016/j.saa.2012.01.051

Notice: *Changes introduced as a result of publishing processes such as copy-editing and formatting may not be reflected in this document. For a definitive version of this work, please refer to the published source:*

<http://dx.doi.org/10.1016/j.saa.2012.01.051>

1 **A vibrational spectroscopic study of planchéite $\text{Cu}_8\text{Si}_8\text{O}_{22}(\text{OH})_4\cdot\text{H}_2\text{O}$**

2
3 **Ray L. Frost,* Yunfei Xi**

4
5 Chemistry Discipline, Faculty of Science and Technology, Queensland University of
6 Technology, GPO Box 2434, Brisbane Queensland 4001, Australia.

7
8
9 **ABSTRACT**

10
11 Planchéite $\text{Cu}_8\text{Si}_8\text{O}_{22}(\text{OH})_4\cdot\text{H}_2\text{O}$ is a hydrated copper hydroxy silicate. The objective of this
12 work is to use Raman and infrared spectroscopy to determine the molecular structure of
13 planchéite. Raman bands of planchéite at around 1048, 1081 and 1127 are described as the ν_1
14 $-\text{SiO}_3$ symmetric stretching vibrations; Raman bands at 828, 906 are attributed to the $\nu_3 -$
15 SiO_3 antisymmetric stretching vibrations. The Raman band at 699 cm^{-1} is assigned to the ν_4
16 bending modes of the $-\text{SiO}_3$ units. The intense Raman band at 3479 cm^{-1} is ascribed to the
17 stretching vibration of the OH units. The Raman band at 3250 cm^{-1} is evidence for water in
18 the structure. A comparison of the spectra of planchéite with that of shattuckite and
19 chrysocolla.

20
21 **Keywords:** planchéite, shattuckite, silicate, Raman spectroscopy, hydroxyl, healing mineral

22
23

* Author to whom correspondence should be addressed (r.frost@qut.edu.au)
P +61 7 3138 2407 F: +61 7 3138 1804

24 **Introduction**

25 The mineral planchéite is a hydrated copper silicate mineral with formula
26 $\text{Cu}_8\text{Si}_8\text{O}_{22}(\text{OH})_4\cdot\text{H}_2\text{O}$ [1]. The two minerals shattuckite $\text{Cu}_5(\text{SiO}_3)_4(\text{OH})_2$ [2] and planchéite
27 were first thought to be the same mineral [3]. However it was proven that the minerals were
28 different [3, 4]. Shattuckite is closely allied to planchéite $\text{Cu}_8\text{Si}_8\text{O}_{22}(\text{OH})_4\cdot\text{H}_2\text{O}$ in structure
29 and appearance [5-7]. The mineral planchéite is orthorhombic of point group $2/m\ 2/m\ 2/m$.
30 The cell data is space group: Pcnb: $a = 19.043(3)$, $b = 20.129(5)$, $c = 5.269(1)$, $Z = 4$. This
31 is the most symmetrical class in the orthorhombic crystal class. Planchéite is a chain silicate
32 with double chains of silica tetrahedra parallel to the C crystal axis. Planchéite occurs as
33 sprays of acicular or fibrous radial clusters, with fibers extended parallel to the chains, i.e.
34 along the C crystal axis. Planchéite is a secondary mineral formed in the oxidized zone of
35 copper ore deposits. The mineral may be associated with other secondary copper minerals
36 including chrysocolla, diopside, conicalcrite, malachite and tenorite.

37

38 Raman spectroscopy has proven very useful for the study of minerals [8, 9]. Indeed, Raman
39 spectroscopy is most useful for the study of diagenetically related minerals as often occurs
40 with minerals containing copper and silicate groups. Yet, there appear to be no Raman or
41 spectroscopic studies of this mineral planchéite. Some infrared [10] and optical studies have
42 been undertaken [11, 12]. This paper is a part of systematic studies of vibrational spectra of
43 minerals of secondary origin in the oxide supergene zone. The objective of this research is to
44 report the Raman spectra of planchéite and to relate the spectra to the molecular structure of
45 the mineral.

46

47 **EXPERIMENTAL**

48

49 **Minerals**

50 The planchéite minerals were supplied by the Mineralogical Research Company. The
51 mineral sample studied in this work originated from Tsumeb, Guchab, Okatumba, about 80
52 km east of Windhoek, Namibia. The type locality of the mineral is the Sanda Mine, Mindouli,
53 Pool Region, Republic of Congo. Details of the mineral have been published (page 651)
54 [13]. Planchéite is also found at the Mt Isa Mines, Mt Isa, Queensland, Australia.
55 Shattuckite from Bisbee, Cochise County, Arizona, was used for spectroscopic purposes in
56 this work. Details of the mineral shattuckite have been published (page 726) [13].

57

58

59 **Raman spectroscopy**

60

61 Crystals of planchéite were placed on a polished metal surface on the stage of an Olympus
62 BHSM microscope, which is equipped with 10x, 20x, and 50x objectives. The microscope is
63 part of a Renishaw 1000 Raman microscope system, which also includes a monochromator, a
64 filter system and a CCD detector (1024 pixels). The Raman spectra were excited by a
65 Spectra-Physics model 127 He-Ne laser producing highly polarised light at 633 nm and
66 collected at a nominal resolution of 2 cm^{-1} and a precision of $\pm 1\text{ cm}^{-1}$ in the range between
67 200 and 4000 cm^{-1} . Repeated acquisitions on the crystals using the highest magnification
68 (50x) were accumulated to improve the signal to noise ratio of the spectra. Spectra were
69 calibrated using the 520.5 cm^{-1} line of a silicon wafer. Previous studies by the authors provide
70 more details of the experimental technique. Alignment of all crystals in a similar orientation
71 has been attempted and achieved. However, differences in intensity may be observed due to
72 minor differences in the crystal orientation.

73

74 **Infrared spectroscopy**

75

76 Infrared spectra were obtained with a Nicolet Nexus 870 FTIR spectrometer with a smart
77 endurance single bounce diamond ATR cell. Spectra over the $4000\text{--}525\text{ cm}^{-1}$ range were
78 obtained by the co-addition of 128 scans with a resolution of 4 cm^{-1} and a mirror velocity of
79 0.6329 cm/s . Spectra were co-added to improve the signal to noise ratio. The infrared spectra
80 are given in the supplementary information.

81

82 Spectral manipulation such as baseline correction/adjustment and smoothing were performed
83 with the Spectracalc software package GRAMS (Galactic Industries Corporation, NH, USA).
84 Band component analysis was undertaken using the Jandel 'Peakfit' software package that
85 enabled the type of fitting function to be selected and allows specific parameters to be fixed
86 or varied accordingly. Band fitting was undertaken using a Lorentzian-Gaussian cross-
87 product function with the minimum number of component bands used for the fitting process.
88 The Gaussian-Lorentzian ratio was maintained at values greater than 0.7 and fitting was
89 undertaken until reproducible results were obtained with squared correlations of r^2 greater

90 than 0.995.

91

92 **RESULTS AND DISCUSSION**

93

94 **Background**

95 The isolated tetrahedral SiO_4 unit has 9 internal modes of which four modes are vibrationally
96 active due to degeneracy. These vibrations are labelled as the ν_1 symmetric stretching mode,
97 the ν_2 doubly degenerate bend, the ν_3 triply degenerate stretching vibration and the ν_4 triply
98 degenerate bending mode. Only the ν_3 and ν_4 modes are infrared active providing the
99 symmetry of the SiO_4 unit is maintained. The values for zircon as an example are ν_1 974, ν_2
100 266 and 439, ν_3 885, 989 and 1008, and ν_4 430, 608 cm^{-1} . The fact that planchéite follows a
101 pyroxene type structure means that the siloxane units for polymeric chains and thus the
102 degeneracy of the vibrational modes above will be lifted. The result of this is that the spectra
103 will show much greater complexity. Two types of oxygens may be distinguished, namely
104 terminal and bridging oxygens. Additional bands should be observed related to the Si-O-Si
105 bending vibrations.

106

107 **Raman spectroscopy**

108 The Raman spectrum over the 100 to 4000 cm^{-1} region is displayed in Figure 1. It is obvious
109 that there are wide spectral regions where no bands are found. Therefore, the spectra are
110 divided into regions based upon the type of vibration being observed. For example, the OH
111 stretching region is observed in the 2700 to 3600 cm^{-1} region. The infrared spectrum of
112 planchéite over the 500 to 4000 cm^{-1} region is displayed in Figure 2. Comparison of the
113 spectra enables the relative intensities of both the Raman and infrared bands to be observed.

114

115 Dowty [14-16] showed the relationship between crystal structure of silicate minerals and their
116 vibrational spectra. Dowty calculated the band positions for the different ideal silicate units.
117 Importantly, the type of structure of silicate minerals can be predicted from the position of the
118 Raman and infrared bands. Dowty showed that the $-\text{SiO}_3$ units had a unique band position of
119 980 cm^{-1} [16] (see Figures 2 and 4 of this reference). Dowty also showed that Si_2O_5 units
120 had a Raman peak at around 1100 cm^{-1} . The Raman spectrum in the 600 to 1400 cm^{-1} region
121 is shown in Figure 3. This spectral region is where the Si-O stretching vibrations are found.
122 The intense sharp band at 1081 cm^{-1} is assigned to the SiO symmetrical stretching vibration.
123 This band according to Dowty is associated with the vibrations of Si_2O_5 units. The shoulder

124 band at 1048 cm^{-1} is also attributed to the SiO symmetrical stretching vibration. The sharp
125 Raman band at around 668 cm^{-1} is assigned to the ν_4 bending mode. The three bands at 828,
126 863 and 906 cm^{-1} are attributed to the ν_3 -SiO₃ antisymmetric stretching vibrations. In
127 comparison, for the mineral shattuckite, a band at around 980 cm^{-1} is observed and attributed
128 to the ν_1 -SiO₃ symmetric stretching vibration. The bands for shattuckite at around 890,
129 1058 and 1102 are described as the ν_3 -SiO₃ antisymmetric stretching vibrations. The fact
130 that shattuckite follows a pyroxene type structure means that the siloxane units for polymeric
131 chains and thus the degeneracy of the vibrational modes above will be lifted. The result of
132 this is that the spectra will show much greater complexity. Two types of oxygens may be
133 distinguished, namely terminal and bridging oxygens. Additional bands should be observed
134 related to the Si-O-Si bending vibrations. The Raman spectrum of shattuckite displays a band
135 at 1043 cm^{-1} with a shoulder band at 1048 cm^{-1} . Dowty's calculations predicted the band at
136 1081 cm^{-1} is attributable to a Si₂O₅ silicate unit [16]. Chrysocolla (Cu,
137 Al)₂H₂Si₂O₅(OH)₄·nH₂O is another hydrated copper hydroxy silicate, the spectra of which
138 may also be used for comparative purposes. The Raman spectrum of chrysocolla displays a
139 Raman band at around 1042 cm^{-1} . This band is attributed to a SiO₃ stretching vibration of
140 silicate. The 1043 cm^{-1} band of shattuckite is in a similar position to the 1042 cm^{-1} of
141 chrysocolla.

142

143 The infrared spectrum of planchéite in the 600 to 1200 cm^{-1} region is reported in Figure 4.
144 Much greater complexity is observed in the infrared spectrum compared with the Raman
145 spectrum. Bands in the Raman spectra are sharp compared with the bands in the infrared
146 spectrum. The sharp bands at 1051 and 1097 cm^{-1} with shoulders at 1037 and 1105 cm^{-1} are
147 assigned to the SiO stretching vibrations. The intense infrared bands in the 740 to 900 cm^{-1}
148 are attributed to the ν_3 antisymmetric -Si-O stretching modes. In comparison, the Raman
149 band for shattuckite at around 670 cm^{-1} is assigned to the ν_4 bending modes of the -SiO₃
150 units. Another shattuckite band is around 785 cm^{-1} . This band is considered to be a Si-O-Si
151 chain stretching mode.

152

153 The Raman spectrum of planchéite in the 100 to 600 cm^{-1} region is reported in Figure 5. The
154 Raman bands at around 384 , 403 and 421 cm^{-1} are attributed to the ν_2 -O-Si-O bending
155 modes. For shattuckite, Raman bands at around 395 and 441 cm^{-1} are attributed to the ν_2
156 bending modes. The Raman bands at 476 and 505 cm^{-1} may be assigned to the ν_4 -O-Si-O
157 bending modes. The Raman bands at 302 and 328 cm^{-1} are associated with CuO stretching

158 vibrations. The Raman bands in the 100 to 245 cm^{-1} may be described as lattice vibrations.
159 The sharp bands at 139 and 186 cm^{-1} may be described as lattice vibrations.

160

161 The Raman spectrum of planchéite in the OH stretching region is reported in Figure 6. The
162 spectrum is dominated by two bands at 3250 and 3479 cm^{-1} . These bands are assigned to the
163 OH stretching vibration of the OH units in the planchéite structure. Other Raman bands are
164 observed at 2864, 2901, 2923 cm^{-1} attributed to strongly hydrogen bonded water molecules.
165 Another Raman band at 3061 cm^{-1} is assigned to water stretching bands. In comparison, the
166 intense sharp band for shattuckite at around 3604 cm^{-1} is assigned to the OH stretching
167 vibration of the OH units in the shattuckite structure. The infrared spectrum of planchéite in
168 the 2400 to 3800 cm^{-1} region is shown in Figure 7. The sharp infrared band at 3498 cm^{-1} is
169 assigned to the OH stretching vibration. A series of bands in the 2400 to 3400 cm^{-1} region
170 are attributed to water stretching vibrations. Strong infrared bands are observed at 3188 and
171 3248 cm^{-1} .

172

173 The Raman spectrum in the 1400 to 1800 cm^{-1} region is displayed in Figure 8. An intense
174 band at 1510 cm^{-1} with a shoulder at 1538 cm^{-1} , is observed and assigned to the hydroxyl
175 deformation vibration. Other bands are observed at 1438, 1452 and 1597 cm^{-1} . The infrared
176 spectrum in this spectral region is shown in Figure 9. Intense bands are observed at 1387 and
177 1514 cm^{-1} with shoulder bands at 1331, 1423 and 1538 cm^{-1} .

178

179 **Conclusions**

180

181 Vibrational spectroscopy has been used to characterise the copper silicate mineral planchéite.
182 Planchéite is one of a number of copper based silicate minerals. There are a significant
183 number of silicate minerals which have copper as one of the main cations. These include
184 kinoite $\text{Ca}_2\text{Cu}_2\text{Si}_3\text{O}_{10}(\text{OH})_4$, chrysocolla $(\text{Cu},\text{Al})_2\text{H}_2\text{Si}_2\text{O}_5(\text{OH})_4 \cdot n\text{H}_2\text{O}$, diopside $\text{CuSiO}_3 \cdot \text{H}_2\text{O}$,
185 planchéite $\text{Cu}_8\text{Si}_8\text{O}_{22}(\text{OH})_4 \cdot \text{H}_2\text{O}$, shattuckite $\text{Cu}_5(\text{SiO}_3)_4(\text{OH})_2$, whelanite
186 $\text{Ca}_5\text{Cu}_2(\text{OH})_2\text{CO}_3 \cdot \text{Si}_6\text{O}_{17} \cdot 4\text{H}_2\text{O}$, ajoite $(\text{K},\text{Na})\text{Cu}_7\text{AlSi}_9\text{O}_{24}(\text{OH})_6 \cdot 3\text{H}_2\text{O}$, apachite
187 $\text{Cu}_9\text{Si}_{10}\text{O}_{29} \cdot 11\text{H}_2\text{O}$, papagoite $\text{CaCuAlSi}_2\text{O}_6(\text{OH})_3$.

188

189 The mineral is a hydrated copper hydroxy silicate $\text{Cu}_8\text{Si}_8\text{O}_{22}(\text{OH})_4 \cdot \text{H}_2\text{O}$. Based upon the
190 vibrational spectroscopy of the hydroxyl stretching region, water is involved in very strong
191 hydrogen bonding in planchéite.

192 Bands attributed to SiO stretching and bending vibrations are identified. The Raman and
193 infrared spectra can be used to distinguish the mineral planchéite from the other copper
194 silicate minerals.

195

196 **Acknowledgments**

197 The financial and infra-structure support of the Queensland University of Technology,
198 Chemistry discipline is gratefully acknowledged. The Australian Research Council (ARC) is
199 thanked for funding the instrumentation.

200

201

202

203 **References**

204

- 205 [1] H.T. Evans, Jr., M.E. Mrose, *American Mineralogist* 62 (1977) 491.
206 [2] F. Zambonini, *Compt. rend.* 166 (1918) 495.
207 [3] W.T. Schaller, *Journal of the Washington Academy of Sciences* 9 (1919) 131.
208 [4] A. Schoep, *Bulletin des Societes Chimiques Belges* 34 (1925) 315.
209 [5] M.T. Le Bihan, *Comptes Rendus des Seances de l'Academie des Sciences, Serie D:*
210 *Sciences Naturelles* 263 (1966) 1801.
211 [6] M.T. Le Bihan, *Bulletin de la Societe Francaise de Mineralogie et de Cristallographie*
212 90 (1967) 3.
213 [7] C. Guillemin, R. Pierrot, *Bulletin de la Societe Francaise de Mineralogie et de*
214 *Cristallographie* 84 (1961) 276.
215 [8] C. Groppo, C. Rinaudo, S. Cairo, D. Gastaldi, R. Compagnoni, *European Journal of*
216 *Mineralogy* 18 (2006) 319.
217 [9] L.A. Haskin, A. Wang, B.L. Jolliff, *Institute of Physics Conference Series* 165 (2000)
218 101.
219 [10] Y.I. Ryskin, G.P. Stavitskaya, N.A. Toropov, *Zhurnal Neorganicheskoi Khimii* 5
220 (1960) 2727.
221 [11] K.B.N. Sarma, B.J. Reddy, S.V.J. Lakshman, *Proceedings of the Nuclear Physics and*
222 *Solid State Physics Symposium* 25C (1984) 209.
223 [12] P. Tarte, *Boletin de la Academia Nacional de Ciencias (Argentina)* 43 (1962) 55.
224 [13] J.W. Anthony, R.A. Bideaux, K.W. Bladh, M.C. Nichols, *Handbook of Mineralogy.*
225 *Mineral Data Publishing, Tuscon, Arizona, USA, 1995.*
226 [14] E. Dowty, *Physics and Chemistry of Minerals* 14 (1987) 542.
227 [15] E. Dowty, *Physics and Chemistry of Minerals* 14 (1987) 122.
228 [16] E. Dowty, *Physics and Chemistry of Minerals* 14 (1987) 80.

229

230

231

232 **List of Figures**

233

234 Figure 1 Raman spectrum of planchéite over the 100 to 4000 cm^{-1} range.

235

236 Figure 2 Infrared spectrum of planchéite over the 500 to 4000 cm^{-1} range.

237

238 Figure 3 Raman spectrum of planchéite over the 600 to 1400 cm^{-1} range.

239

240 Figure 4 Infrared spectrum of planchéite over the 600 to 1200 cm^{-1} range.

241

242 Figure 5 Raman spectrum of planchéite over the 100 to 600 cm^{-1} range.

243

244 Figure 6 Raman spectrum of planchéite over the 2600 to 3800 cm^{-1} range.

245

246 Figure 7 Infrared spectrum of planchéite over the 2400 to 3800 cm^{-1} range.

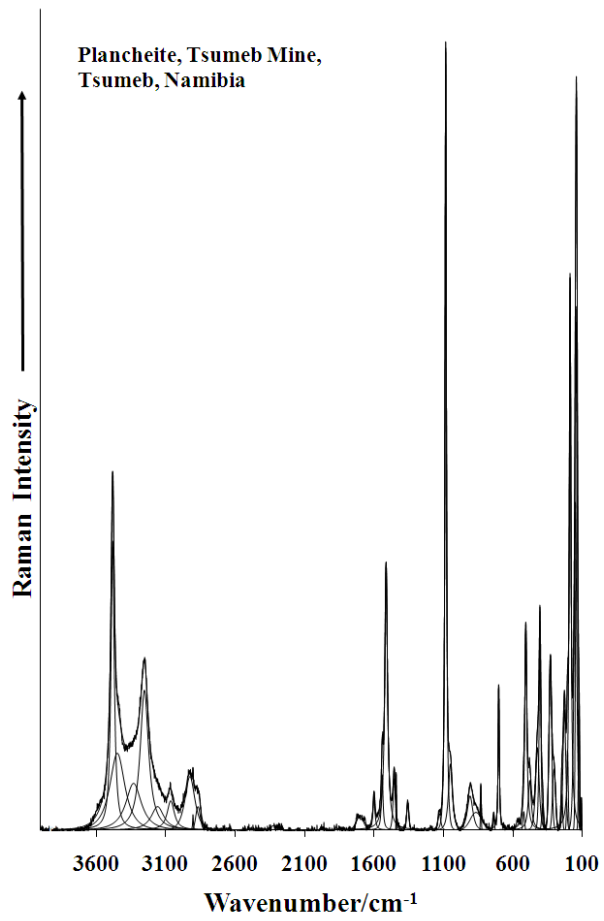
247

248 Figure 8 Raman spectrum of planchéite over the 1400 to 1800 cm^{-1} range.

249

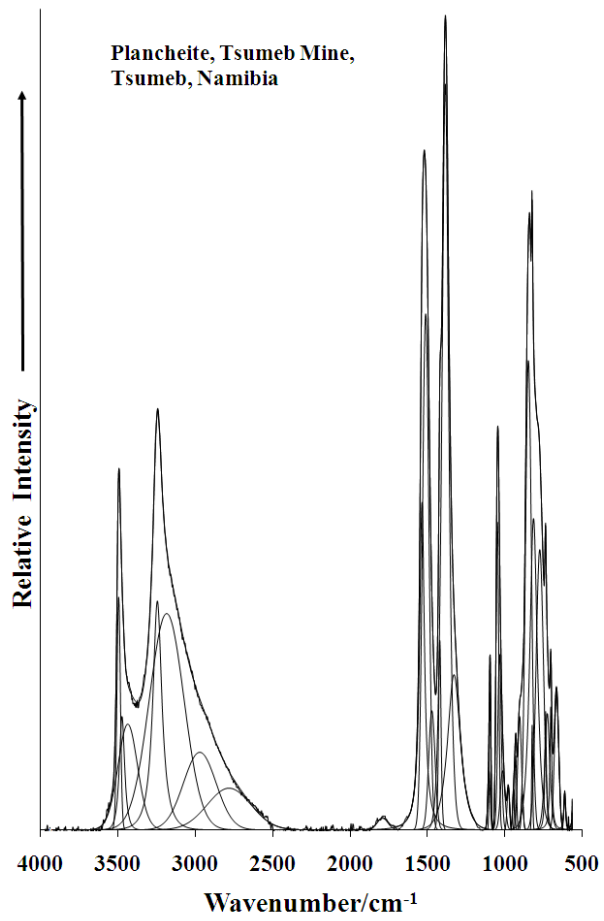
250 Figure 9 Infrared spectrum of planchéite over the 1200 to 1900 cm^{-1} range.

251



252
253
254
255

Figure 1

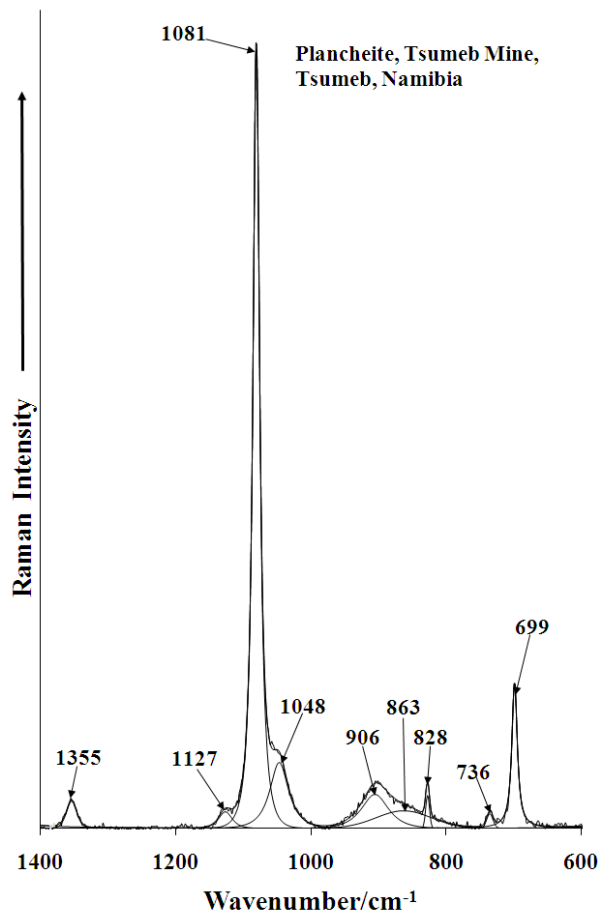


256

257

258 **Figure 2**

259



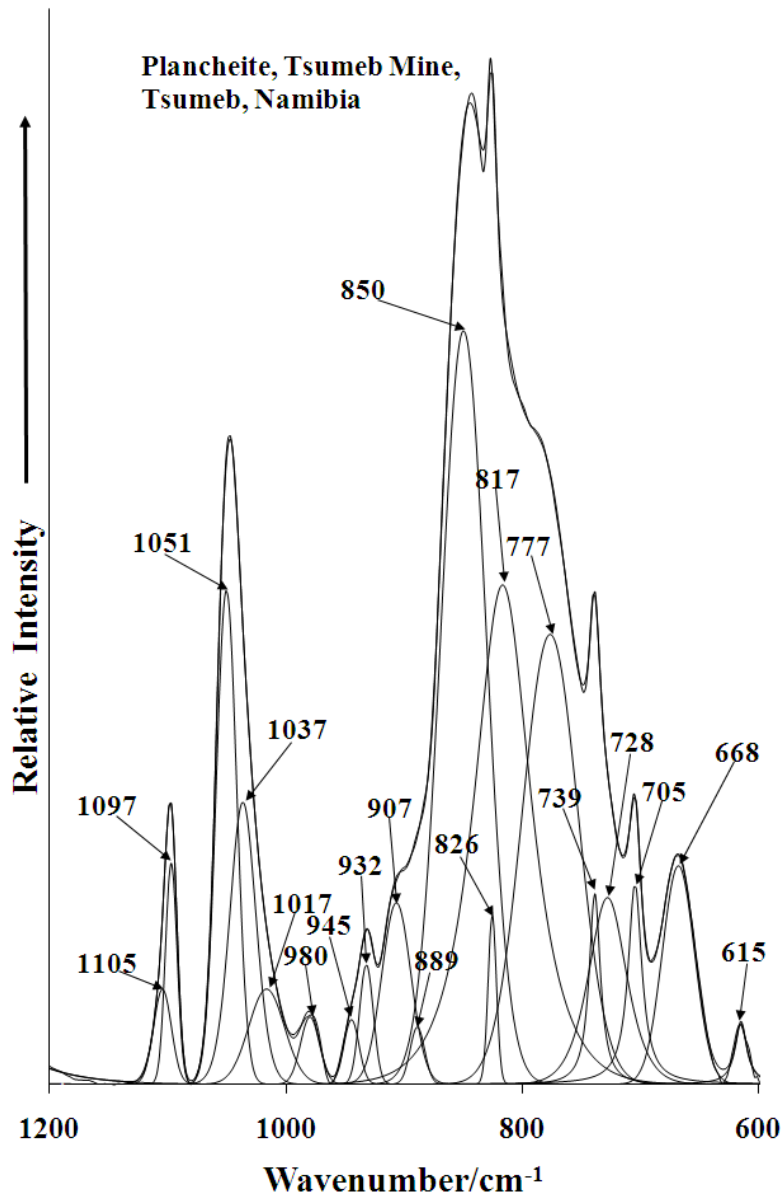
260

261

262 **Figure 3**

263

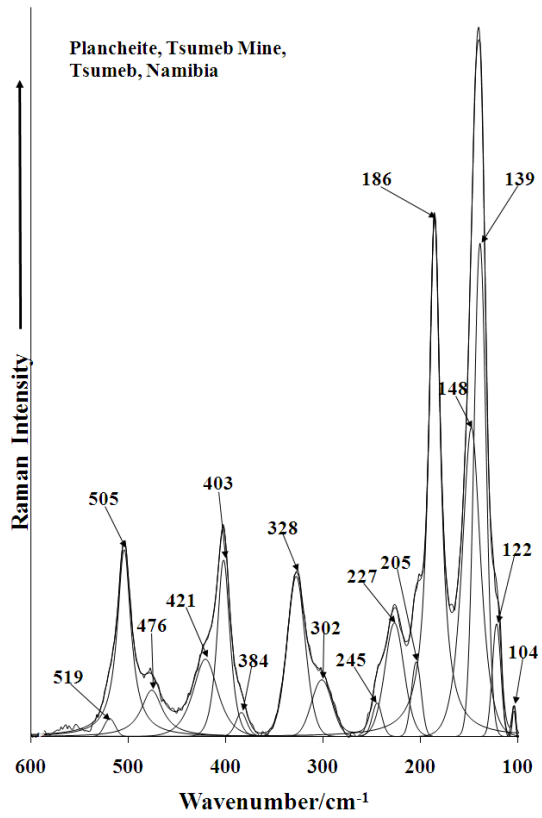
264



265

266

267 **Figure 4**



268

269

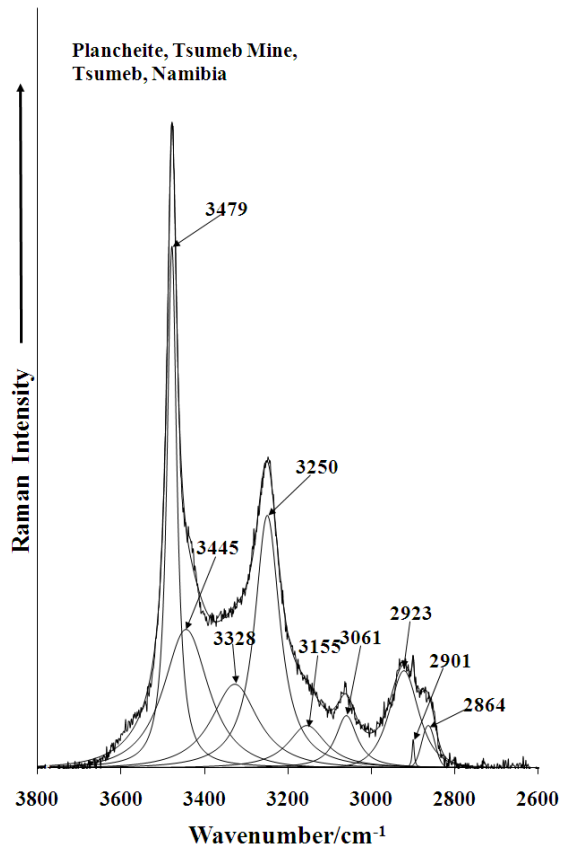
270 **Figure 5**

271

272

273

274



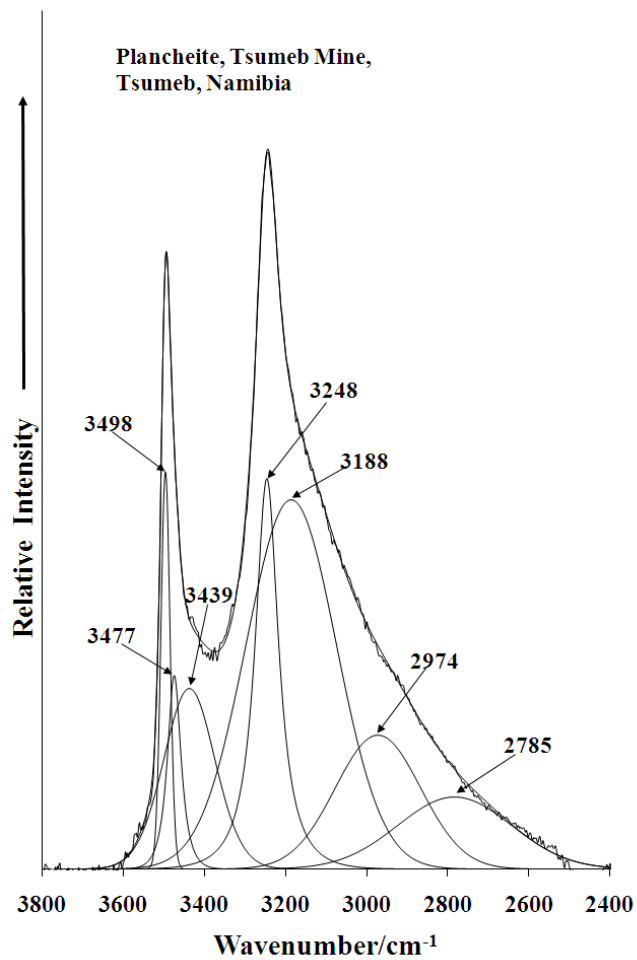
275

276

277 **Figure 6**

278

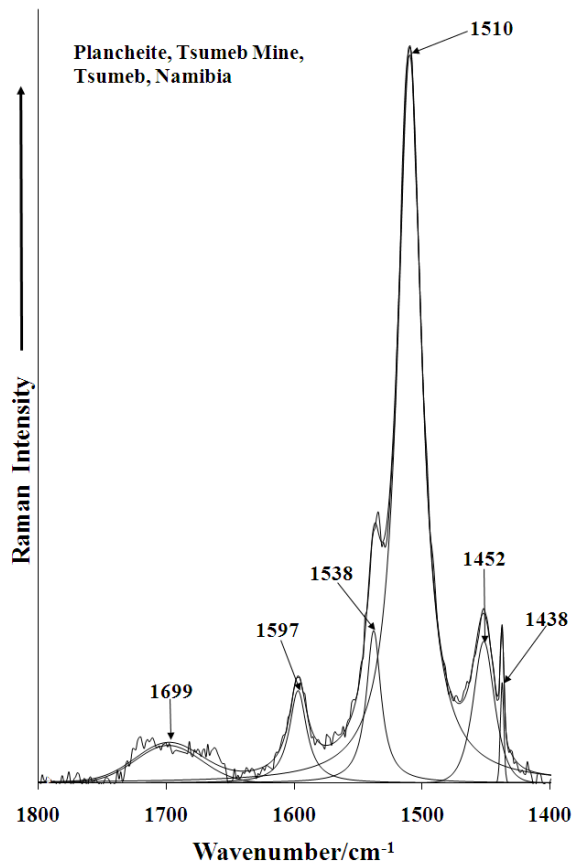
279



280

281

282 **Figure 7**



283

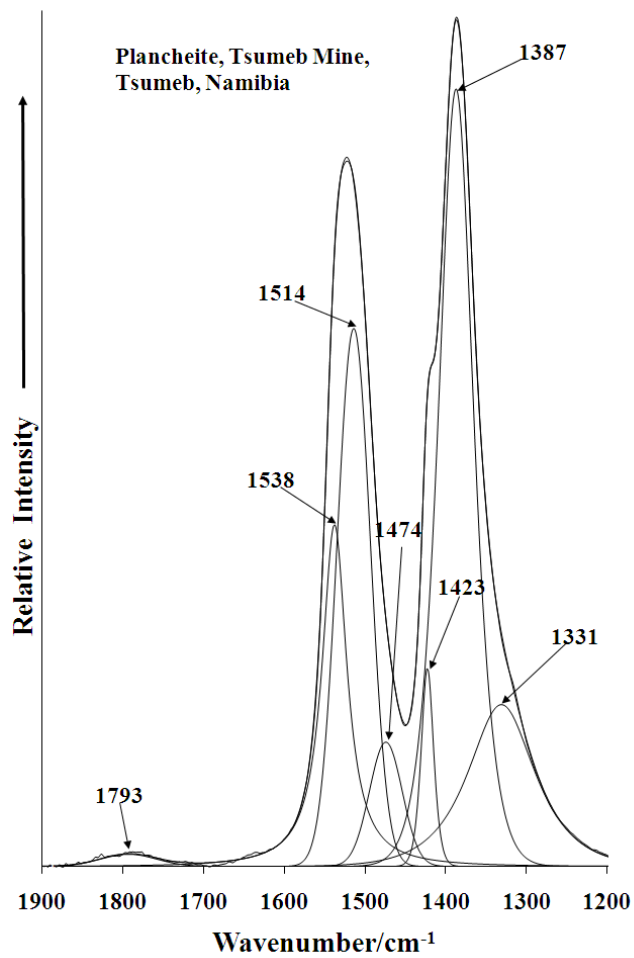
284

285 **Figure 8**

286

287

288



289

290

291 **Figure 9**